Protein Science (1995), *4*:35–43. Cambridge University Press. Printed in the USA.

Conformational stability of HPr: The histidine-containing phosphocarrier protein from *Bacillus subtilis*

J. MARTIN SCHOLTZ

Department of Medical Biochemistry & Genetics, Center for Macromolecular Design, Texas A&M University, College Station, Texas 77843-1114

(RECEIVED October 7, 1994; ACCEPTED November 10, 1994)

Abstract

The conformational stability of the histidine-containing phosphocarrier protein (HPr) from *Bacillus subtilis* has been determined using a combination of thermal unfolding and solvent denaturation experiments. The urea-induced denaturation of HPr was monitored spectroscopically at fixed temperatures and thermal unfolding was performed in the presence of fixed concentrations of urea. These data were analyzed in several different ways to afford a measure of the cardinal parameters (ΔH_g, T_g, ΔS_g, and ΔC_p) that describe the thermodynamics of folding for HPr. The method of Pace and Laurents (Pace CN, Laurents DV, 1989, *Biochemistry 28*:2520–2525) was used to estimate ΔC_p as was a global analysis of the thermal- and urea-induced unfolding data. Each method used to analyze the data gives a similar value for ΔC_p (1,170 ± 50 cal mol^{-1} K^{-1}). Despite the high melting temperature for HPr (T_g = 73.5 °C), the maximum stability of the protein, which occurs at 26 °C, is quite modest (ΔG_s = 4.2 kcal mol^{-1}). In the presence of moderate concentrations of urea, HPr exhibits cold denaturation, and thus a complete stability curve for HPr, including a measure of ΔC_p, can be achieved using the method of Chen and Schellman (Chen B, Schellman JA, 1989, *Biochemistry 28*:685–691). A comparison of the different methods for the analysis of solvent denaturation curves is provided and the effects of urea on the thermal stability of this small globular protein are discussed. The methods presented will be of general utility in the characterization of the stability curve for many small proteins.

Keywords: cold denaturation; conformational stability; protein folding

A complete thermodynamic description of the stability of globular proteins is crucial to our understanding of the energetics of protein structure, folding, and function. Here we describe the complete stability curve, the variation of the Gibbs energy of folding with temperature, for histidine-containing phosphocarrier protein (HPr) using a combination of thermal- and urea-induced unfolding experiments and spectroscopic probes for the folding transition. The data have been analyzed in several ways to afford measures of the cardinal thermodynamic parameters (ΔH_g, ΔS_g, T_g, etc., evaluated at the temperature where ΔG = 0; see Becktel & Schellman, 1987) necessary for a description of the conformational stability of HPr. Included in the analysis is the assumption that ΔC_p is temperature independent and that the denatured forms of HPr at high temperature or in the presence of high concentrations of urea are thermodynamically indistinguishable. These two assumptions allow a global analysis of the stability of HPr as functions of both temperature and urea concentration. The simplicity of this model will be presented and the potential problems will be addressed.

HPr is a small globular protein with no disulfides or other prosthetic groups. HPr is a phosphocarrier protein in the phosphoenolpyruvate-dependent carbohydrate transport system (PTS) in bacteria (reviewed by Meadow et al., 1990). The three-dimensional structures of HPr from a variety of bacterial sources have been determined by crystallographic (*Bacillus subtilis*, Herzberg et al., 1992; *Escherichia coli*, Jia et al., 1993b; and *Streptococcus faecalis*, Jia et al., 1993a) and NMR techniques (*B. subtilis*, Wittekind et al., 1992; *E. coli*, Klevit & Waygood, 1986; Hammen et al., 1991; van Nuland et al., 1992, 1994; and *Staphylococcus aureus*, Kalbitzer et al., 1991; Kalbitzer & Hengstenberg, 1993). The proteins from these sources have identical folding topologies with two or three α-helices on one face of a four-stranded, antiparallel β-sheet. The HPr proteins have been the subject of a number of biochemical studies regarding the function of the protein in the PTS. Here we report the

Reprint requests to: J. Martin Scholtz, Department of Medical Biochemistry & Genetics, 440 Reynolds Building, Texas A&M University, College Station, Texas 77843-1114; e-mail: jm-scholtz@tamu.edu.

thermodynamic stability of the wild-type HPr protein from *B. subtilis*.

To determine the conformational stability of *B. subtilis* HPr, we employ two perturbants, temperature and urea, as a way to induce protein unfolding. The results are analyzed with several models for the effects of temperature and urea on protein stability and a few general points emerge. We address the possible contribution of the enthalpy of denaturant binding in thermal unfolding curves in the presence of urea and test the assumptions of the temperature- and denaturant-independence to ΔC_p for HPr folding. The results and methods are of general utility in the characterization of the conformational stability of small globular proteins.

Results

The conformational stability of HPr at pH 7.0 in 10 mM potassium phosphate has been determined using a combination of thermal unfolding curves in the presence of various concentrations of urea or by urea-denaturation curves at various temperatures. The results of the thermal unfolding experiments, as monitored by the change in ellipticity at 222 nm by CD, are shown in Figure 1. The addition of increasing concentrations of urea causes the high temperature transition to occur at lower temperatures and reveals low-temperature denaturation at urea concentrations greater than 2 M. All transitions are fully reversible as evidenced by the coincidence of the data obtained from heating the samples and from cooling the samples, provided the protein solution is not allowed to remain at temperatures >80 °C for more than 1 h. Upon prolonged exposure to high temperatures, especially in the presence of urea, some reversibility is lost, presumably due to irreversible aggregation or modification of the protein by urea decomposition products (data not shown).

The results of several of the urea-denaturation experiments at constant temperature are shown in Figure 2. Again, the onset of cold denaturation is evident by the decrease in the midpoint of the cooperative unfolding transition as the temperature is lowered. These transitions are also reversible and, furthermore, the equilibration of the folded and unfolded forms of the protein is extremely rapid. The latter observation allowed us to perform the denaturation experiments using the two different

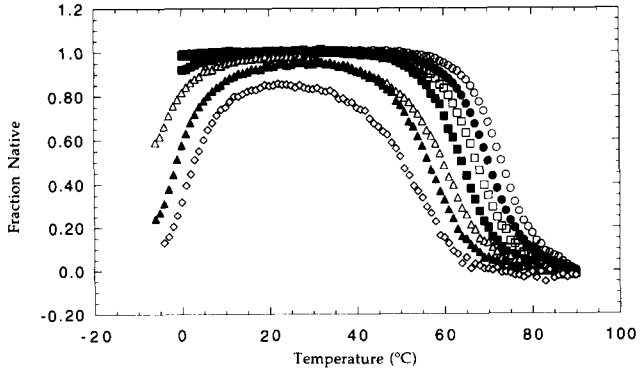

Fig. 1. Thermal unfolding curves for HPr in various concentrations of urea at pH 7.0 (10 mM potassium phosphate) as monitored by the change in ellipticity at 222 nm. The concentration of urea in each sample is: ○, 0 M; ●, 0.5 M; □, 1 M; ■, 1.5 M; △, 2 M; ▲, 2.5 M; ◇, 3 M.

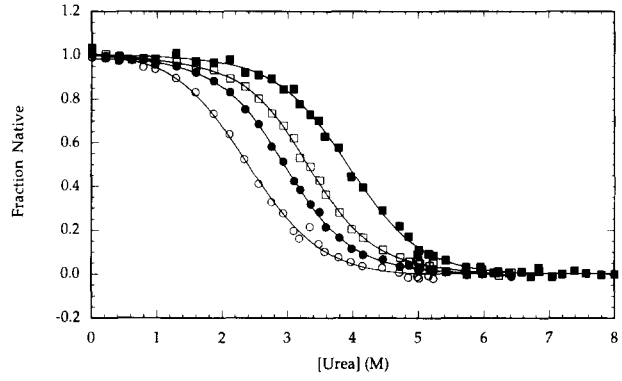

Fig. 2. Urea-denaturation curves at various temperatures at pH 7.0 (10 mM potassium phosphate) as monitored by the change in ellipticity at 222 nm. Temperatures are: ■, 25 °C; □, 10 °C; ●, 5 °C; ○, 0 °C. Lines through the data are the fit of the LEM (Equation 1) using parameters listed in Table 1.

protocols described in the Materials and methods. Examples of both types of experiments are shown in Figure 2. Denaturation experiments at 0 and 25 °C were performed using independent samples for each urea concentration, whereas the other experiments illustrate the serial addition of a concentrated urea solution to the sample in the cuvette with a correction for the volume increase. Each protocol gives good results; however, the serial addition method is superior in terms of the amount of protein required for a complete denaturation curve and in the elimination of systematic errors associated with preparing several independent samples.

To convert the measured ellipticity at 222 nm to the fraction of native protein (f_N) shown in Figures 1 and 2, the CD baselines for the fully folded and denatured forms of the protein were determined as a function of temperature and urea concentration. Linear expressions for the baselines as functions of temperature or urea concentration, obtained by measuring the changes in ellipticity in the pre- and post-transition regions of the curves, were combined to give the native and denatured planes for the three-dimensional analysis of the data. Alternatively, these baseplanes were determined from a global analysis of the data. Each method gives similar results, and, furthermore, the cardinal parameters defining the stability curve are insensitive to the observed variation in the baseline parameters provided by the different methods of determination. The best estimates for the native and unfolded baseplanes using the representations given by Equations 8 and 9 (see the Materials and methods) provide:

$$[\theta]_N(T,[\text{urea}]) = -10{,}500 + 8.5 \cdot T - 23 \cdot [\text{urea}]$$

$$[\theta]_D(T,[\text{urea}]) = -1{,}970 - 4.5 \cdot T + 360 \cdot [\text{urea}],$$

with $[\theta]_x$ in deg cm^2 dmol^{-1}, T in °C and [urea] in M. These relationships are used to determine f_N for each experiment in Figures 1 and 2 using Equation 10 (see the Materials and methods for details).

The chief parameter needed for a complete analysis of the stability curve for protein folding is the change in heat capacity, ΔC_p, for the transition. To determine this parameter and the others needed for a full description of the stability curve for HPr

(Becktel & Schellman, 1987), the data in Figures 1 and 2 were analyzed in several different ways: (1) the method of Pace and Laurents (1989) was used with the thermal unfolding data in the absence of urea along with the nine urea-denaturation curves in Figure 2 and Table 1; (2) the method of Chen and Schellman (1989) was applied to the thermal unfolding data in the presence of 3 M urea; (3) the variation in T_g and ΔH_g as a function of urea concentration (Fig. 1) was used to determine ΔC_p; and (4) a global analysis of the data was performed (see below). Each method of analysis assumes a two-state transition (N ⇌ U) with the equilibrium constant (K_{eq}) defined as the ratio of fraction unfolded to fraction folded. Evidence for the two-state unfolding reaction was provided by the coincidence of the thermal unfolding curves using different probes for the transition including near- and far-UV CD and the presence of an isodichroic point at ≈205 nm in the CD spectra recorded at different temperatures (data not shown).

The urea-denaturation curves shown in Figure 2 were analyzed with the linear extrapolation method (LEM) following the procedures described by Pace (1986) and Santoro and Bolen (1992). The alternative methods of analysis of urea-denaturation curves are discussed below (see Discussion). For the LEM, the data in the transition regions of the urea-denaturation curves were fit to the equation:

$$\Delta G_{obs} = \Delta G_{water} - m \cdot [\text{urea}]. \quad (1)$$

This method assumes a linear relationship (m-value) between ΔG^0 of folding and the molar concentration of urea. Table 1 shows the results for the nine different urea-denaturation curves performed at different temperatures; the lines in Figure 2 show the results of the fit of each individual experiment at the indicated temperature. It should be noted that the m-values are temperature-independent over the entire 40° range of temperatures. This temperature independence is discussed below.

The thermal unfolding curves presented in Figure 1 were analyzed in several ways. For the data in the absence of urea, a van't Hoff analysis was used to calculate ΔH_g and T_g from the data in the transition region. As expected, over the narrow temperature range of the transition with the small ΔC_p for HPr (see below), we could not detect any curvature in the plot of $\ln K_{eq}$ as a function of $1/T$, and thus ΔC_p could not be determined directly from this single experiment. To determine ΔC_p, the method of Pace and Laurents (1989) was employed. With this method, the nine ΔG_{water} values (Equation 1) from the urea-denaturation curves at low temperatures (Fig. 2; Table 1) were combined with the data in the transition region of the thermal unfolding curve in the absence of urea and analyzed with a modified version of the Gibbs–Helmholtz equation:

$$\Delta G(T) = \Delta H_g(1 - T/T_g) - \Delta C_p[(T_g - T) + T \cdot \ln(T/T_g)]. \quad (2)$$

The results of the nonlinear least-squares fit of the data to Equation 2 are shown in Figure 3 and Table 2. The ΔC_p calculated in this manner is 1,160 ± 50 cal mol^{-1} K^{-1}.

The variation of ΔH_g with temperature afforded by the addition of urea (Fig. 1) can also be used to calculate ΔC_p using a van't Hoff analysis of the individual unfolding curves. The slope of the plot of ΔH_g versus T_g, shown in Figure 4 (solid points and solid line), gives a second measure of ΔC_p (1,170 ± 80 cal mol^{-1} K^{-1}). This result is also shown in Table 2. The potential contribution of the enthalpy of urea binding and an analysis of this contribution to the observed conformational enthalpy change for HPr is discussed below.

In addition to using a series of either thermal unfolding curves or urea-denaturation curves to provide a measure of ΔC_p, we have employed the method first described by Chen and Schellman (1989) to analyze the single thermal unfolding curve in the presence of 3.0 M urea. The thermal transition reveals both high- and low-temperature unfolding and, thus, the complete stability curve can be obtained. This analysis, which assumes a temperature-independent ΔC_p, provides an excellent check on this assumption of our model as well as providing evidence for the denaturant-independence of ΔC_p. The single transition curve covers a large temperature range where ΔG changes from positive to negative and passes through zero twice.

Table 1. *Analysis of urea-denaturation curves*

Temperature (°C)	C_{mid} (M urea)	m-value (cal mol^{-1} M^{-1})	ΔG_{water} (kcal mol^{-1})
0	2.38	1,080	2.57
5	2.95	1,040	3.07
10	3.32	1,040	3.45
15	3.52	1,060	3.73
20	3.88	1,020	3.96
25	3.90	1,080	4.21
30	3.92	1,030	4.04
35	3.77	1,050	3.96
40	3.64	1,040	3.79

[a] The data in the transition regions of the nine urea-denaturation curves were fit to the linear extrapolation model provided by Equation 1 using the method of Santoro and Bolen (1988). Errors on the C_{mid} values are ±0.05 M, ±40–50 cal mol^{-1} M^{-1} for the m-values, and ±0.10–0.15 kcal mol^{-1} for ΔG_{water}.

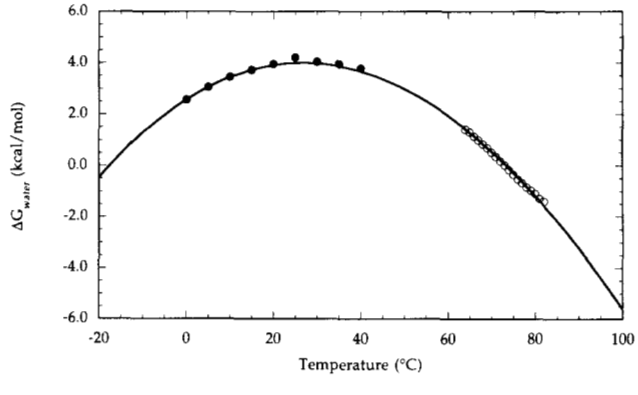

Fig. 3. HPr stability curve determined using the method of Pace and Laurents (1989). The data at lower temperatures (0–40 °C) are from the results of the urea-denaturation curves (Table 1), and the data at higher temperatures are from the thermal unfolding curve in the absence of urea (Fig. 1). The best-fit parameters describing the stability of HPr are shown in Table 2.

Table 2. *Thermodynamic parameters for the folding of HPr*

Parameter	Pace and Laurents[a]	Global fit[b]	ΔH_g versus T_g analysis		Chen and Schellman[e]
			ΔH_g (obs)[c]	ΔH_g (calc)[d]	
ΔC_p (cal mol^{-1} K^{-1})	1,160 ± 50	1,160 ± 50	1,170 ± 80	1,100 ± 100	1,190 ± 50
ΔH_g (kcal mol^{-1})	58.1 ± 1.7	59.2 ± 2.5			
ΔS_g (cal mol^{-1} K^{-1})	168 ± 5	171 ± 6			
T_g (°C)	73.4 ± 0.2	73.8 ± 0.4			
m (cal mol^{-1} M^{-1})		1,050 ± 50			

[a] The method of Pace and Laurents (1989) was used to calculate the stability curve using the nine urea-denaturation curves at lower temperatures and the single thermal unfolding curve in the absence of urea.
[b] Equation 4 was used to provide a global analysis of the data in the transition regions of the curves shown in Figures 1 and 2.
[c] The variation of ΔH_g with T_g as a function of urea concentration was used to calculate ΔC_p (Fig. 4).
[d] The ΔH_g values were corrected for the effect of the enthalpy of urea binding using Equations 5, 6, and 7 (see Fig. 4).
[e] The method of Chen and Schellman (1989) was used to analyze the single thermal unfolding curve in the presence of 3 M urea (Fig. 5). The errors represent one standard deviation of the indicated value as described in the text.

The Gibbs-Helmholtz equation, written in terms of constant coefficients, is used to fit these data:

$$\ln K' = A + B\cdot(T_0/T) + C\cdot\ln(T_0/T) \qquad (3)$$

with

$$A = -[\Delta C_p' + \Delta S'(T_0)]/R$$

$$B = [\Delta C_p' - \Delta S'(T_0)]/R - \Delta G'(T_0)/RT_0$$

$$C = -\Delta C_p'/R,$$

where T_0 is an arbitrary reference temperature and the primes indicate the thermodynamic values in the presence of 3 M urea. If T_0 corresponds to either of the transition temperatures, then $\Delta G' = 0$ by definition and $A = -B$. We have employed the method of Chen and Schellman (1989) in which T_0 is varied until $A = -B$ for both the high- and low-temperature unfolding transitions. Each transition gives the same value for the coefficient C and hence ΔC_p. Figure 5 shows the nonlinear least-squares fit for the thermal unfolding curve in the presence of urea using this method. The ΔC_p calculated from this analysis, 1,190 ± 50 cal mol^{-1} K^{-1}, is shown in Table 2. The fit is quite good (variance = 0.0056) and provides evidence for the temperature-independence of ΔC_p.

The final method used to analyze the urea-denaturation and thermal-unfolding data presented in Figures 1 and 2 employs a global fit to all the data. The three-dimensional analysis uses the LEM (Equation 1) in combination with the Gibbs-Helmholtz relationship (Equation 2). Combining these equations gives:

$$\Delta G(T,[\text{urea}]) = \Delta H_g(1 - T/T_g) - \Delta C_p[(T_g - T) + T\cdot\ln(T/T_g)] - m\cdot[\text{urea}]. \qquad (4)$$

Equation 4 was fitted to the data in the transition regions ($0.05 \le f_N \le 0.95$) of the thermal- and urea-induced unfolding curves with ΔH_g, T_g, ΔC_p, and m as variable parameters. The

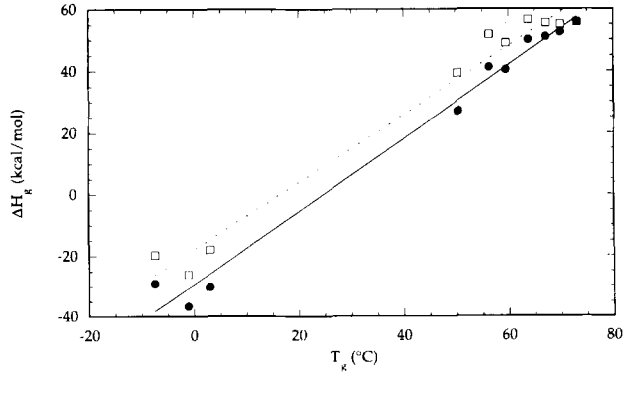

Fig. 4. The variation of ΔH_g with T_g from the thermal unfolding data in the presence of different concentrations of urea (Fig. 1). Solid points (●) and line (——) represent the observed ΔH_g values at the indicated melting temperatures (T_g) and provide ΔC_p = 1,170 ± 80 cal mol^{-1} K^{-1}; open symbols (□) and dashed line (--) represent the data corrected for the enthalpy of urea binding (see text) and give ΔC_p = 1,100 ± 100 cal mol^{-1} K^{-1}.

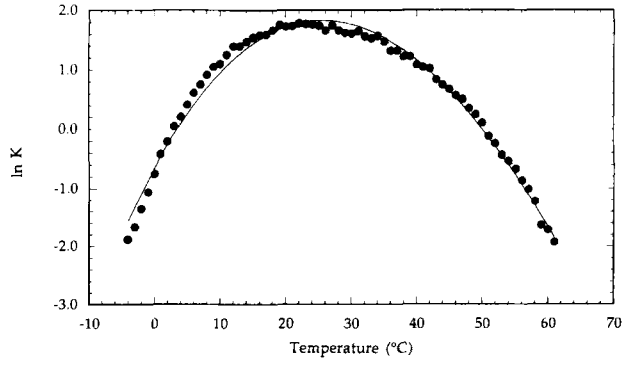

Fig. 5. Analysis of the thermal unfolding data for HPr in the presence of 3 M urea as described by Chen and Schellman (1989). The best-fit ΔC_p value is 1,190 ± 50 cal mol^{-1} K^{-1} for both the heat- and cold-denaturation processes (see text).

results of the nonlinear least-squares fit are shown in Table 2 and Figure 6. The plots at various urea concentrations in Figure 6 are offset by $m \cdot$ [urea] for clarity. There is good agreement between the calculated curves and the data (symbols) over the entire range of temperature and urea concentration, suggesting that the relationships employed, namely temperature-independent ΔC_p and m-values, are valid.

As a further test for the temperature-independent m-value for the effect of urea on the stability of HPr, the data in Figure 1 have been used to calculate m-values at temperatures within the transition region for the thermal unfolding curves. By taking isothermal slices through the data in Figure 1 and plotting the observed ΔG as a function of urea concentration, slopes or m-values ranging from 1,120 to 920 cal mol^{-1} M^{-1} are found for all temperatures between 54 and 73 °C (data not shown). There is a slight temperature dependence to these m-values; however, the mean value in this temperature range is identical to the m-values determined from the LEM analysis of the urea-denaturation experiments at lower temperatures (Fig. 2; Table 1). The excellent agreement provides further evidence for the temperature-independence of the m-value for the effect of urea on the stability of HPr.

Discussion

A complete description of the conformational stability of a protein as a function of temperature represents the stability curve. This complete description allows one to calculate the stability of a protein at any temperature using the Gibbs-Helmholtz relationship (Equation 2). Here we provide a description of the stability curve for *B. subtilis* HPr using a combination of thermal and urea-induced unfolding. There are three principal results: (1) The data are consistent with our assumption of thermodynamically indistinguishable denatured states at either high temperature or in concentrated urea. (2) Furthermore, the data

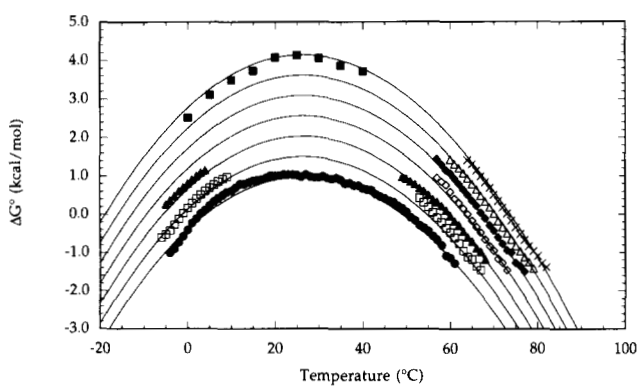

Fig. 6. A global analysis of the data in the transition regions of the thermal- and urea-denaturation curves shown in Figures 1 and 2. The best-fit parameters used to construct the curves (——) are shown in Table 2. The data from thermal unfolding curves at the indicated urea concentration are: ×, 0 M; △, 0.5 M; ◆, 1 M; ◇, 1.5 M; ▲, 2 M; □, 2.5 M; ●, 3 M. Data from the urea-denaturation curves at constant temperature are represented in this plot by the ΔG_{water} values (■) from Table 1 for clarity, although the data from entire urea-denaturation curves were used in the global analysis (see text). The thermal unfolding curves at different urea concentrations are offset in this plot by $m \cdot$ [urea], where m = 1,050 cal mol^{-1} M^{-1}.

are consistent with temperature-independent ΔC_p and m-values over the large temperature range of the unfolding transitions. (3) In moderate concentrations of urea, HPr exhibits cold denaturation and thus a complete stability curve can be obtained by a single thermal unfolding experiment in the presence of urea.

The equilibrium unfolding of HPr has been monitored by a spectroscopic probe (CD) and the resulting data analyzed with a simple two-state unfolding reaction. Although we do observe an isodichroic point in the CD spectra of HPr through the thermal unfolding transitions (≈205 nm, data not shown), a similar isodichroic point cannot be demonstrated for the urea-denaturation process because we are unable to obtain CD data below 210 due to the large absorbance of urea. One of the major assumptions of the analysis is that the thermally unfolded form and the denatured form of HPr in urea are thermodynamically equivalent and the difference in the spectroscopic measure of ellipticity can be regarded as a simple baseline effect. For example, the observed CD signal at 222 nm of the two denatured forms of HPr are not identical: $[\theta]_{obs}$ at 90 °C and no urea is approximately −2,500 deg cm^2 dmol^{-1}, whereas $[\theta]_{obs}$ in 8 M urea, 0 °C is near 0. (For comparison, $[\theta]_{obs}$ for the folded protein in the absence of urea at 0 °C is −10,500 deg cm^2 dmol^{-1}.) All the available data indicate that we can treat this difference in the CD signals of the unfolded forms of the protein as a simple baseline or baseplane effect.

It is known that thermally denatured proteins often show a "residual" CD signal near 220 nm (see Privalov et al., 1989; Robertson & Baldwin, 1991, and references therein), yet appear to be devoid of stable hydrogen bonded secondary structure as evidenced by the lack of protected amide protons (Loftus et al., 1986; Robertson & Baldwin, 1991) and appear to be completely unfolded using direct calorimetric measurements (Privalov et al., 1989). What is important for the present analysis is whether the two unfolded forms of HPr, obtained either at high temperature or at lower temperatures in the presence of high concentrations of urea, are thermodynamically equivalent despite the fact that a spectroscopic probe for structure gives a different absolute measure for the unfolded forms. Several studies on other proteins have indicated that this assumption is valid. Santoro and Bolen (1992) have used a combination of solvent denaturation curves and direct calorimetric measurements of the stability of thioredoxin in the presence of guanidine hydrochloride and find complete agreement between the ΔG^0 values for protein stability determined with the various techniques. The same conclusions have been reached for turkey ovomucoid third domain (Swint & Robertson, 1993) and for ribonuclease T1 (Pace, 1990; Yu et al., 1994). Not only are the Gibbs energy changes identical for the direct calorimetric techniques and the spectroscopic methods employed here, but the enthalpy, entropy, and heat capacity changes that accompany the transition are also identical for a number of different proteins if the denaturant solvation is correctly taken into account (Pfiel & Privalov, 1976; Privalov et al., 1989; Makhatadze & Privalov, 1992). This latter point is discussed below for the case of HPr.

The use of two different perturbants, temperature and urea, allows a description of the stability of HPr over a wide range of both temperature and urea concentration. In order to provide a global analysis of the data, two critical observations were made: namely that ΔC_p (Equation 2) and the m-value (Equation 1) are temperature independent. Therefore, the LEM (Equation 1) can be combined with the Gibbs-Helmholtz rela-

tionship (Equation 2) to provide the simple relationship describing the conformational stability at every temperature and urea concentration (Equation 4). The assumptions used in Equation 4 can be tested using the available data. For example, the analysis of the single thermal unfolding curve in the presence of 3 M urea shows both high- and low-temperature unfolding (Fig. 5) and the constant ΔC_p model (Equation 3) can describe the data using the method first described by Chen and Schellman (1989). This analysis provides a good check on the constant ΔC_p model because $\Delta G'$ is determined over a wide range of temperatures in a single experiment. The good agreement between the best-fit curve and the data provides support for the temperature independence of ΔC_p over the temperature range available. The slight deviation between the best-fit curve and the data, especially at lower temperatures, may suggest that ΔC_p is not temperature independent; however, the deviation is small and well within the error associated with the determination of the CD baselines.

The second observation is that the m-value for the effect of urea on the conformational stability of HPr is temperature independent. This observation is supported by two results. First, the nine urea-denaturation curves at temperatures from 0 to 40 °C provide, with error, identical measures of the m-value (Table 1) and, furthermore, these values, along with the LEM, are able to describe the observed data very well (Fig. 2). Second, m-values at higher temperatures can be determined by replotting the data in the transition regions of the thermal unfolding curves in Figure 1. These m-values at temperatures between 54 and 73 °C, where there are four or more data points to define the line, do show a slight variation with temperature; however, the dependence is small and the m-values are within the range seen at lower temperatures (Table 1). Taken together, these two observations allow us to express the conformational stability of HPr, at all temperatures and urea concentrations, using the simple expression in Equation 4.

The temperature-independent m-value for HPr must be a result of compensating temperature effects. This can be demonstrated by analyzing the urea-denaturation data (Fig. 2; Table 1) with the thermodynamic binding model for the action of urea on proteins (Schellman, 1955, 1987; Aune & Tanford, 1969):

$$\Delta G^0 = \Delta G_{water} - RT \cdot \Delta n \cdot \ln(1 + k \cdot a), \quad (5)$$

where Δn is the number of new, independent binding sites for urea in the unfolded form of the protein, k is the binding constant for urea to these new sites, and a is the activity of the urea solution, usually expressed as molar activity. To reconcile the temperature-independent m-value, either Δn, k, or a must have compensating temperature dependencies. The molar activity, a, of aqueous urea solutions does increase with temperature (Stokes, 1967) and there is a negative enthalpy of urea binding to proteins and peptides (Schellman, 1955; Robinson & Jencks, 1965; Schonert & Stroth, 1981; Makhatadze & Privalov, 1992) and, hence, k decreases with temperature. Therefore, it appears that, at least for the temperatures for which experimental data are available, a temperature-independent m-value may result simply from the compensating temperature effects on k and urea activity. In addition to this explanation, Δn may show a temperature dependence. The data for the urea denaturation of HPr have been analyzed with the binding model (Equation 5), and indeed we find temperature-dependent Δn values, ranging from $\Delta n = 40$ at 0 °C to $\Delta n = 31$ at 40 °C (data not shown). Together, the temperature dependence of Δn, k, and a must cancel and thus we find, for HPr, a temperature-independent m-value for urea at all accessible temperatures.

Thermodynamic stability of B. subtilis HPr

The cardinal parameters required for a description of the thermodynamic stability of HPr are shown in Table 2. Together with the Gibbs–Helmholtz relationship, these parameters can be used to determine the conformational stability of HPr at any temperature, and for HPr, at any urea concentration using Equation 4. The chief parameter needed for the analysis is ΔC_p, the change in heat capacity for the unfolding reaction. The determination of ΔC_p from the data in Figures 1 and 2 represents the primary result of this analysis. We have employed four different methods to analyze the data and arrive at identical measures of ΔC_p (Table 2): 1,170 ± 50 cal mol^{-1} K^{-1}. This value is independent of temperature and able to describe the heat- and cold-denaturation of HPr. Also, ΔC_p is independent of urea concentration and thus a single ΔC_p is able to describe the transitions in the absence and presence of urea.

The analysis of the thermal unfolding curves in the presence of different concentrations of urea also affords one measure of ΔC_p (Fig. 4; Table 2). Perturbation of T_g with denaturant has been suggested in the past (Foss & Schellman, 1959; Schellman, 1990; Santoro & Bolen, 1992; Swint & Robertson, 1993) as a way to determine ΔC_p; however, calorimetric and other studies have suggested that ΔC_p in the presence of denaturant is expected to be higher than in water (Pfiel & Privalov, 1976; Privalov et al., 1989; Makhatadze & Privalov, 1992). This results from the sign of the enthalpy associated with denaturant binding and the proportionality of the binding enthalpy with denaturant concentration (Schellman, 1955; Robinson & Jencks, 1965; Schonert & Stroth, 1981; Makhatadze & Privalov, 1992). Separating the observed ΔH_g into the enthalpy change for the protein conformational change ($\Delta H_{g,conf}$) and the enthalpy of denaturant binding ($\Delta H_{g,urea}$) provides:

$$\Delta H_{g,obs} = \Delta H_{g,conf} + \Delta H_{g,urea}. \quad (6)$$

Following the procedure described by Makhatadze and Privalov (1992), the $\Delta H_{g,urea}$ contribution can be expressed as:

$$\Delta H_{g,urea} = \Delta h \cdot \Delta n \cdot \frac{k \cdot a}{1 + k \cdot a}, \quad (7)$$

where Δh is the enthalpy of urea binding to a single "site" on the protein, Δn is the number of new "sites" exposed upon protein unfolding, and the ratio $k \cdot a/(1 + k \cdot a)$ provides the occupancy of the site. This analysis follows directly from the thermodynamic binding model for the action of urea on proteins provided by Equation 5.

We have analyzed the thermal unfolding data in the presence of urea with Equations 5, 6, and 7 to estimate the contribution of the enthalpy of urea binding to the observed enthalpy change for the transition. In this analysis we have used $\Delta n = 40$, the largest value determined at low temperatures, $k = 0.06$ and $\Delta h = -2.11$ kcal mol^{-1} as described by Makhatadze and Privalov (1992). This will overestimate the contribution of

$\Delta H_{g,urea}$ to the observed ΔH_g because both Δn and k decrease with temperature; however, it is nonetheless useful to calculate the upper limit for $\Delta H_{g,urea}$. The resulting value of $\Delta H_{g,urea}$ (Equation 7) can be used with Equation 6 to determine the contribution of urea binding to the observed enthalpy change. The adjusted values are shown in Figure 4 (open symbols and dashed line). The ΔC_p calculated from the slope of this line, 1,100 ± 100 cal mol^{-1} K^{-1}, is within error of the value calculated from the raw data. This suggests that the ΔC_p value is independent of urea concentration and thus the simple relationship used in Equation 4 is valid for HPr. Further evidence for the urea independence of ΔC_p for HPr comes from a comparison of the value determined from the thermal unfolding transition in 3 M urea (Fig. 5) with the values determined from other methods of analysis (Table 2).

The cardinal parameters able to describe the conformational stability of HPr are shown in Table 2. These values, along with the complete thermodynamic analysis, provide some interesting comparisons to other proteins. First, the ΔC_p value is typical for small globular proteins when considered on a per residue basis (Privalov & Gill, 1988; Alexander et al., 1992). Second, despite the relatively high T_g (73.4 ± 0.2 °C), the global stability of HPr at lower temperatures is quite modest (ΔG_s = 4.2 kcal mol^{-1} at ≈26 °C). In fact, this stability is only about $7RT$, indicating that 1 in every 1,200 HPr molecules is unfolded at 26 °C. This result seems at odds with hydrogen exchange studies (Wittekind et al., 1992) that find a few backbone amide hydrogens in HPr with half-times for exchange approaching a day. If these persistent hydrogens can exchange only out of the globally unfolded form of the protein (Kim & Woodward, 1993; Bai et al., 1994), the global conformational stability of HPr would be about twice that found here (Bai et al., 1993). Further studies on the mechanism of hydrogen exchange from native proteins is required before a complete understanding of this apparent contradiction can be realized (Kim & Woodward, 1993; Bai et al., 1994).

The high T_g and a small ΔG_s found here for HPr unfolding is the direct consequence of the small ΔC_p and ΔH_g. A related comparison has been presented by Alexander et al. (1992) for another small protein, the B1 domain of protein G, and this may be a general result for all small proteins. Together, the observations of a typical ΔC_p and relatively small ΔH_g provide the criteria for the observation of cold denaturation. Although we do not observe cold denaturation in the absence of urea, it is clear that HPr is less stable at 0 °C than at 25 °C (Fig. 2; Table 1). In the presence of low concentrations of urea, the onset of cold denaturation is observed and, in 3 M urea, almost complete unfolding occurs at low temperature. This results directly from the thermodynamic parameters for HPr and the relationship describing the stability curve for protein folding (Equation 4).

Although it is not possible to prove unequivocally the assumptions of temperature-independent ΔC_p and m-values, the evidence cited above, together with the ability of Equation 4 to describe the data adequately, suggest that the assumptions are valid for the HPr system described here. The generality of the approach for other proteins, or even with other denaturants and HPr, remains an open question, one that we are actively pursuing because the simplicity of this approach makes it possible to determine the complete stability for a protein with a minimum of effort.

Materials and methods

The expression of *B. subtilis* HPr was performed in *E. coli* as described by Reizer et al. (1989). The *E. coli* strain harboring the wild-type *B. subtilis* HPr gene (*ptsH*) on the pRE plasmid was a generous gift of J. Reizer and M.H. Saier, Jr. In our hands, the expression and purification procedure provided ca. 50 mg of homogeneous HPr from 4 L of late logarithmic cells. Protein purity was judged to be greater than 95% from denaturing gel electrophoresis as described previously (Reizer et al., 1989). The purified protein was dialyzed extensively against several changes of distilled water prior to preparing samples for spectroscopic analysis. Protein concentration of the stock solution was determined using the absorbance of the two tyrosine residues in HPr and the extinction coefficients in water and 6 M GuHCl given by Brandts and Kaplan (1973), 2,780 and 2,900 M^{-1} cm^{-1} at 275 nm, respectively.

CD at 222 nm was used to monitor the equilibrium unfolding data using an Aviv 62DS spectropolarimeter equipped with a temperature control and stirring unit. The thermal unfolding curves were performed with heating rates from 15 to 90 °C per hour in cuvettes with pathlengths of 1 or 10 mm. The reversibility of the thermal transitions was checked in each case by recording scans obtained upon cooling the solution from 90 to 0 °C immediately after the conclusion of the thermal transition. In all cases, the transitions were independent of the rate of heating, ≥95% reversible, and independent of protein concentration. Some reversibility was lost upon prolonged exposure of the sample to high temperature, especially in the presence of urea. This irreversibility is presumably due to chemical modification of the protein by the products of urea decomposition.

The urea-denaturation curves at constant temperature were performed with two different protocols. In both cases, urea solutions were prepared fresh daily in buffered solutions containing 10 mM potassium phosphate at pH 7.0 and the concentration of the urea stock solution was determined by refractive index measurements (Pace, 1986). The first method for determining the urea-denaturation curve employed individual samples at various urea concentrations that were allowed to equilibrate in a circulating water bath overnight. Each independent sample was placed in the CD instrument and the signal recorded after averaging for 200 s. The alternative method was developed after our finding of the rapid equilibration of the folding transition. In this method, small aliquots of concentrated urea in buffer were added directly to the protein sample in the cuvette and allowed to reach thermal and chemical equilibrium before recording the CD signal. Serial additions of urea were made to the same protein sample, and the protein concentration was corrected for the increase in volume. This alternative method is superior in terms of the elimination of errors associated with the preparation of independent samples, as well as the need for much less protein for a single unfolding transition curve. Examples of both methods are presented in the Results.

The complete analysis of the denaturation data, including both thermal- and urea-induced denaturation experiments, requires an accurate determination of the pre- and posttransition baselines and planes defined as:

$$[\theta]_N(T,[\text{urea}]) = [\theta]_N(0°,0\text{ M}) + a_N\cdot[\text{urea}] + b_N\cdot T \quad (8)$$

$$[\theta]_D(T,[\text{urea}]) = [\theta]_D(0°,0\text{ M}) + a_D\cdot[\text{urea}] + b_D\cdot T, \quad (9)$$

where the first term in each equation is the CD value for the native and denatured forms, respectively, of the protein at 0 °C in the absence of urea. The second terms give the linear slopes of the CD values with temperature, whereas the final term shows the urea effects of the baselines. Taken as a whole, each of the Equations 8 and 9 defines two planes for the pre- and posttransition regions of urea-temperature space. The fraction of native protein at any temperature and concentration of urea, f_N, can be determined from the observed CD signal using:

$$f_N = \frac{[\theta]_{obs}(T,[\text{urea}]) - [\theta]_D(T,[\text{urea}])}{[\theta]_N(T,[\text{urea}]) - [\theta]_D(T,[\text{urea}])}. \quad (10)$$

For most of the unfolding transitions, Equations 8 and 9 reduce to a simple two-term linear representation of the baselines that can be measured independently for each transition and combined to provide the entire baseplanes. In the cases where the pretransition baseline was ill-defined or completely absent, such as the thermal unfolding curve in 3.0 M urea, the baseline could be determined by comparing the thermal unfolding data with the urea-denaturation curves at constant temperatures. Alternatively, the data for the necessary regions of the baseplanes from all of the experiments could be combined and fit to Equation 8 or 9 to determine the best-fit slopes and intercepts. Finally, a global analysis of the data, combining Equations 8, 9, and 10 with Equation 4, is used to determine the baseplane parameters as well as the cardinal values for the conformational stability. Each method provides nearly identical values for the baseplane parameters, and, furthermore, the cardinal values describing the conformational stability in Equation 4 are insensitive to the slight variation in baseplane parameters determined by the different methods.

The nonlinear least-squares fitting employed the algorithm that is based on the method described by Johnson and Frasier (1985) and implemented for the Macintosh computer (Brenstein, 1991). Best-fit parameters and their confidence intervals expressed as one standard deviation are given for each fit. A minimum of two repetitions of a given experiment was used in all cases. For the analysis of a transition curve with well-defined baselines, a modification of the method of Santoro and Bolen (1988) was used, using the curve-fitting methods in the KaleidaGraph software (Synergy Software, PCS Inc.). A single urea-denaturation curve can be fit to the equation:

$$[\theta]_{obs} = \frac{([\theta]_N + a_N[\text{urea}]) + ([\theta]_D + a_D[\text{urea}]) \cdot \exp[m \cdot ([\text{urea}] - C_{mid})/RT]}{1 + \exp[m \cdot ([\text{urea}] - C_{mid})/RT]}, \quad (11)$$

with $[\theta]_N$, a_N, $[\theta]_D$, a_D, m, and C_{mid} as fitting parameters. This expression combines the LEM (Equation 1), where $\Delta G_{water} = m \cdot C_{mid}$, and the two-state assumption for the unfolding reaction. The nonlinear least-squares fit of Equation 11 to the data in Figure 2 are shown as the solid lines.

Acknowledgments

This work was supported by a grant from the Robert A. Welch foundation (A-1281). I thank Buzz Baldwin, Doug Barrick, Nick Pace, Andy Robertson, and John Schellman for many helpful discussions; Jonathan Reizer and Milton Saier for the cloned source of *B. subtilis* HPr; and Rachel Klevit for a gift of purified HPr for the initial studies and for her constant encouragement throughout this work.

References

Alexander P, Fahnestock S, Lee T, Orban J, Bryan P. 1992. Thermodynamic analysis of the folding of the streptococcal protein G IgG-binding domains B1 and B2: Why small proteins tend to have high denaturation temperatures. *Biochemistry 31*:3597–3603.

Aune K, Tanford C. 1969. Thermodynamics of the denaturation of lysozyme by guanidine hydrochloride. II. Dependence on denaturant concentration at 25°. *Biochemistry 8*:4586–4590.

Bai Y, Milne JS, Mayne L, Englander SW. 1993. Primary structure effects on peptide group hydrogen exchange. *Proteins Struct Funct Genet 17*:75–86.

Bai Y, Milne JS, Mayne L, Englander SW. 1994. Protein stability parameters measured by hydrogen exchange. *Proteins Struct Funct Genet 20*:4–14.

Becktel WJ, Schellman JA. 1987. Protein stability curves. *Biopolymers 26*:1859–1877.

Brandts JR, Kaplan KJ. 1973. Derivative spectroscopy applied to tyrosyl chromophores. Studies on ribonuclease, lima bean inhibitor, insulin, and pancreatic trypsin inhibitor. *Biochemistry 12*:2011–2024.

Brenstein RJ. 1991. *NonLin for Macintosh*. Carbondale, Illinois: Robelko Software.

Chen B, Schellman JA. 1989. Low-temperature unfolding of a mutant of phage T4 lysozyme. 1. Equilibrium studies. *Biochemistry 28*:685–691.

Foss JG, Schellman JA. 1959. The thermal transition of ribonuclease in urea solutions. *J Phys Chem 63*:2007–2012.

Hammen PK, Waygood EB, Klevit RE. 1991. Reexamination of the secondary and tertiary structure of histidine-containing protein from *Escherichia coli* by homonuclear and heteronuclear NMR spectroscopy. *Biochemistry 30*:11842–11850.

Herzberg O, Reddy P, Sutrina S, Saier M, Reizer J, Kapadia G. 1992. Structure of the histidine-containing phosphocarrier protein HPr from *Bacillus subtilis* at 2.0 Å resolution. *Proc Natl Acad Sci USA 89*:2499–2503.

Jia X, Vandonselaar M, Quail JW, Delbaere LTJ. 1993a. Active-centre torsion-angle strain revealed in 1.6 Å resolution structure of histidine-containing phosphocarrier protein. *Nature 361*:94–97.

Jia Z, Quail JW, Waygood EB, Delbaere LTJ. 1993b. The 2.0-Å resolution structure of *Escherichia coli* histidine-containing phosphocarrier protein HPr. *J Biol Chem 268*:22490–22501.

Johnson MJ, Frasier SG. 1985. Nonlinear least-squares analysis. *Methods Enzymol 117*:301–342.

Kalbitzer HR, Hengstenberg W. 1993. The solution structure of the histidine-containing protein (HPr) from *Staphylococcus aureus* as determined by two-dimensional ^{1}H-NMR spectroscopy. *Eur J Biochem 216*:205–214.

Kalbitzer HR, Neidig KP, Hengstenberg W. 1991. Two-dimensional ^{1}H NMR studies on HPr protein from *Staphylococcus aureus*: Complete sequential assignments and secondary structure. *Biochemistry 30*:11186–11192.

Kim KS, Woodward CK. 1993. Protein internal flexibility and global stability: Effect of urea on hydrogen exchange rates of bovine pancreatic trypsin inhibitor. *Biochemistry 32*:9609–9613.

Klevit RE, Waygood EB. 1986. Two-dimensional ^{1}H NMR studies of histidine-containing protein from *Escherichia coli*. 3. Secondary and tertiary structure as determined by NMR. *Biochemistry 25*:7774–7781.

Loftus D, Gbenle GO, Kim PS, Baldwin RL. 1986. Effects of denaturants on amide proton exchange rates: A test for structure in protein fragments and folding intermediates. *Biochemistry 25*:1428–1436.

Makhatadze GI, Privalov PL. 1992. Protein interactions with urea and guanidinium chloride: A calorimetric study. *J Mol Biol 226*:491–505.

Meadow ND, Fox DK, Roseman S. 1990. The bacterial phosphoenolpyruvate:glucose phosphotransferase system. *Annu Rev Biochem 59*:497–542.

Pace CN. 1986. Determination and analysis of urea and guanidine hydrochloride denaturation curves. *Methods Enzymol 131*:266–280.

Pace CN. 1990. Conformational stability of globular proteins. *Trends Biochem Sci 15*:14–17.

Pace CN, Laurents DV. 1989. A new method for determining the heat capacity change for protein folding. *Biochemistry 28*:2520–2525.

Pfiel W, Privalov PL. 1976. Thermodynamic investigations of proteins. *Biophys Chem 4*:33–40.

Privalov PL, Gill SJ. 1988. Stability of protein structure and hydrophobic interaction. *Adv Protein Chem 39*:191–234.

Privalov PL, Tiktopulo EI, Venyaminov SY, Griko YV, Makhatadze GI, Khechinashvili NN. 1989. Heat capacity and conformation of proteins in the denatured state. *J Mol Biol 205*:737–750.

Reizer J, Sutrina SL, Saier MH Jr, Stewart GC, Peterkofsky A, Reddy P. 1989. Mechanistic and physiological consequences of HPr(ser) phosphorylation on the activities of the phosphoenolpyruvate:sugar phosphotransferase system in gram-positive bacteria: Studies with site-specific mutants of HPr. *EMBO J 8*:2111–2120.

Robertson AD, Baldwin RL. 1991. Hydrogen exchange in thermally denatured ribonuclease A. *Biochemistry 30*:9907–9914.

Robinson DR, Jencks WP. 1965. The effect of compounds on the urea-guanidinium class on the activity coefficient of acetyltetraglycine ethyl ester and related compounds. *J Am Chem Soc 87*:2462–2470.

Santoro MM, Bolen DW. 1988. Unfolding free energy changes determined by the linear extrapolation method. 1. Unfolding of phenylmethanesulfonyl α-chymotrypsin using different denaturants. *Biochemistry 27*: 8063–8068.

Santoro MM, Bolen DW. 1992. A test of the linear extrapolation of unfolding free energy changes over an extended denaturant concentration range. *Biochemistry 31*:4901–4907.

Schellman JA. 1955. The thermodynamics of urea solutions and the heat of formation of the peptide hydrogen bond. *C R Trav Lab Carlsberg Ser Chim 29*:223–229.

Schellman JA. 1987. Selective binding and solvent denaturation. *Biopolymers 26*:549–559.

Schellman JA. 1990. A simple model for solvation in mixed solvents. Applications to the stabilization and destabilization of macromolecular structures. *Biophys Chem 37*:121–140.

Schonert H, Stroth L. 1981. Thermodynamic interaction between urea and the peptide group in aqueous solution at 25 °C. *Biopolymers 20*:817–831.

Stokes RH. 1967. Thermodynamics of aqueous urea solutions. *Aust J Chem 20*:2087–2100.

Swint L, Robertson AD. 1993. Thermodynamics of unfolding for turkey ovomucoid third domain: Thermal and chemical denaturation. *Protein Sci 2*:2037–2049.

van Nuland NAJ, Grötzinger J, Dijkstra K, Scheek RM, Robillard GT. 1992. Determination of the three-dimensional solution structure of the histidine-containing phosphocarrier protein HPr from *Escherichia coli* using multidimensional NMR spectroscopy. *Eur J Biochem 210*:881–891.

van Nuland NAJ, Hangyi IW, van Schaik RC, Berendsen HJC, van Gunsteren WF, Scheek RM, Robillard GT. 1994. The high-resolution structure of the histidine-containing phosphocarrier protein HPr from *Escherichia coli* determined by restrained molecular dynamics from nuclear magnetic resonance nuclear Overhauser effect data. *J Mol Biol 237*:554–559.

Wittekind M, Rajagopal P, Branchini BR, Reizer J, Saier MH Jr, Klevit RE. 1992. Solution structure of the phosphocarrier protein HPr from *Bacillus subtilis* by two-dimensional NMR spectroscopy. *Protein Sci 1*:1363–1376.

Yu Y, Makhatadze GI, Pace CN, Privalov PL. 1994. Energetics of ribonuclease T1 structure. *Biochemistry 33*:3312–3319.